Iranian Journal of Basic Medical Sciences
ijbms.mums.ac.ir

Synergistic induction of apoptosis in cancer cells by combined silver nanoparticles and paclitaxel

Alireza Shams [1]*, Mohammad Amin Shams [2], Maryam Amirinejad [3], Ghazale Molaverdi [4]

[1] Department of Anatomy, School of Medicine, Alborz University of Medical Sciences, Karaj, Iran
[2] School of Medicine, Iran University of Medical Sciences, Tehran, Iran
[3] Department of Anatomy, School of Medicine, Alborz University of Medical Sciences, Karaj, Iran
[4] Dietary Supplements and Probiotic Research Center, Alborz University of Medical Sciences, Karaj, Iran

ARTICLE INFO

Article type:
Original

Article history:
Received: Aug 26, 2025
Accepted: Nov 30, 2025

Keywords:
Apoptosis
HeLa cells
Nanoparticles
Paclitaxel
Silver
Uterine cervical neoplasms

ABSTRACT

Objective(s): Even with treatment, cervical cancer continues to be rampant among females and has the highest mortality. Carrier system therapies, which combine cancer drugs with nanoparticles, are purported to arrest tumor growth and minimize the side effects of cancer drugs. We envisioned paclitaxel-loaded silver nanoparticles (PTX-AgNPs) as an appropriate carrier for targeting cancer cells. Hence, we studied the effects of paclitaxel (PTX) and silver nanoparticles (AgNPs) as an adjunct therapy in the management of cervical cancer.

Materials and Methods: Anti-cancer activity with PTX alone or in combination with AgNPs was assessed by MTT assay and real-time PCR. The mechanism underlying the antiproliferative effects was investigated by measuring the expression of apoptotic markers (Bax, Caspase-3, Bak) and anti-apoptotic markers (Bcl-2, Mcl-1) by RT-PCR.

Results: PTX and silver nanoparticles alone induced apoptosis; however, at lower doses, they showed synergism, with an inhibitory concentration of 50% (IC_{50}). Real-time PCR showed that the combination treatment, PTX and AgNPs, significantly increased the mRNA expression of the Bax, Bak, and Caspase-3 genes in the HeLa cell line compared with mono-treatment ($P<0.05$). Anti-apoptotic Bcl-2 and Mcl-1 mRNA levels were also decreased in all treated groups as compared to control cells.

Conclusion: We showed that silver nanoparticles have a synergistic effect with PTX and were able to give favorable results (higher cell death in the combined group) at lower concentrations of PTX.

▶Please cite this article as:
Shams AR, Shams MA, Amirinejad M, Molaverdi Gh. Synergistic induction of apoptosis in cancer cells by combined silver nanoparticles and paclitaxel. Iran J Basic Med Sci 2026; 29: 634-640. doi: https://dx.doi.org/10.22038/ijbms.2026.90764.19567

Introduction

Cancer is the second most common cause of death, after heart disease, and is characterized by uncontrolled cell growth. About 200 different forms of cancer have been identified, most of which occur in developing countries (1). Cervical cancer is one of the most common diseases in women, predominantly occurring in middle-aged and older women, and it poses the highest mortality rate (2). Due to bad lifestyle choices and habits, the trend of lower age of patients suffering from cervical cancer is showing an alarming downward trend. Very early stages of this type of cancer usually do not demonstrate any specific type of symptom. Over time, it presents symptoms such as vaginal bleeding, pelvic pain, and pain during sex (3). Although modern medical methods are abundant, current treatments for cervical cancer are relatively rare, and the therapeutic effect is limited **(4).** However, nanotechnology was introduced to advance the goals of next-generation cancer research and treatment. Nanoparticles (NPs) can induce apoptosis and affect metastasis *in vitro* and *in vivo* (5). NPs exhibit potent anticancer effects, either by inducing apoptosis in cancer cells or by inhibiting metastasis. NPs initiate apoptosis by generation of reactive oxygen species (ROS), mitochondrial stress, and activation of pro-apoptotic factors leading to the ultimate activation of caspases-3/7 and programmed cell death (6). Simultaneously, NPs inhibit metastasis by inhibiting matrix metalloproteinase (MMP) expression, reducing cell migration/invasion, and disrupting tumor cell adhesion to the extracellular matrix, thereby preventing further spread of the tumor (7). NPs act to recognize molecular markers on the surface of cancer cells. They are often used in biological approaches, such as tumor removal in combination with immunotherapy. NPs were used to deliver anticancer agents for breast and cervical cancers (8). Among the various metal NPs, silver nanoparticles (AgNPs) have been singled out as the most versatile. They are typically chemically stable and exhibit good electrical conductivity, as well as catalytic, antibacterial, anti-inflammatory, and antiviral properties (9). AgNPs have been used as cytotoxic agents against a number of cancer cell lines. AgNP-based cancer treatment mechanisms include immediate cellular damage caused by compromising membrane integrity,

***Corresponding author:** Alireza Shams. Department of Anatomy, School of Medicine, Alborz University of Medical Sciences, Karaj, Iran. Email dr.shams@abzums.ac.ir

oxidative stress, and apoptosis within the treated cells (10). Moreover, they express apoptotic-related genes, such as Bcl-2-Associated X (Bax), B-cell lymphoma 2 (Bcl-2), Caspase 3, and p53, as well as cell-cycle arrest genes. It was stated that AgNPs induce apoptosis in HCT116 and HeLa cells via upregulation of Bcl-2 and P53 (11).

Paclitaxel (PTX) is an anticancer pharmaceutical agent that causes effects on cancer cells of interference with growth, proliferation, and dissemination within the body by its application in treating ovarian, breast, and lung cancers, among others (12). Its mechanisms of action involve microtubule stabilization and polymerization inhibition, which inhibit mitosis during interphase and thereby induce apoptosis (13). One of the mediating factors involved in apoptosis is myeloid cell leukemia sequence 1 (Mcl-1). Mcl-1 is an anti-apoptotic protein that interacts with the apoptosis-inducing proteins Bcl-2 Antagonist/Killer (Bak) and Bax, thereby conferring anti-apoptotic effects. Mcl-1 levels decrease during PTX-induced mitotic arrest, thereby favoring cell death (14). The application of PTX is, however, limited because of its hydrophobic nature, leading to low bioavailability in aqueous solvents (15). Nanocarriers have thus emerged as a promising alternative to address the shortcomings of PTX. Based on the information presented in this study, we intended to investigate the simultaneous effect of PTX and AgNPs on the proliferation of HeLa cancer cells. It may reduce the side effects of the chemotherapy drug PTX.

Materials and Methods

Chemicals

Nanosilver synthesis

The procedure involved the preparation of AgNPs via chemical reduction: 50 ml of 0.0002 M silver nitrate solution was incubated at 30 °C for 20 min, after which 2 ml of 1% sodium citrate solution was added. The above mixture is heated at 80 °C for 10 min. Afterward, 10 µl of 0.1 M sodium borohydride solution was added. The final solution was maintained under the same conditions for a period of 30 min (16). Finally, the resulting powder was diluted into culture medium and used. The necessary tests (SEM, FTIR) for characterizing NPs were carried out after the synthesis of AgNPs.

Loading of paclitaxel drug into silver nanoparticles

Initially, 1 mg of AgNPs was dispersed in 10 ml of sterile distilled water. In a separate step, 6 mg/ml of PTX was dissolved in 2 ml of sterile distilled water, serving as the vehicle. Then, the mixture was poured into AgNPs and stirred for an additional 24 hr. The solution was centrifuged at 6000 rpm, and the precipitate was collected (17). Furthermore, thermo-spectroscopy analysis and scanning electron microscope images of the drug-loaded AgNPs were conducted.

Thermogravimetric analysis (TGA) of synthesized nanoparticles

The analysis of the synthesized NPs included thermal gravimetric analysis (TGA) of the acquired samples. TGA analyses of the samples were carried out using a Linseis STAPT1000 by heating them in air from room temperature to 700 °C at a heating rate of 10 °C per minute (18). Continuous measurements will be carried out of mass loss due to water decomposition and of mass gain due to absorption or oxidation in the present analysis.

Fourier transform infrared spectroscopy (FTIR)

FTIR spectroscopy was used to authenticate the charged silver NPs. For this purpose, the spectrum of pure AgNPs was compared with that of the ones loaded with the drug (19). The presence of benzamide groups was confirmed on the AgNPs.

SEM analysis of AgNPs

Images of original AgNPs and drug-loaded silver NPs were examined with appropriate magnification of a scanning electron microscope (SEM) (20).

Study of drug release from paclitaxel-loaded silver nanoparticles by UV–Vis spectrometer

For the release studies, seven samples of drug-loaded NPs were prepared at a concentration of 1 mg/ml in microtubes. The microtubes were then incubated at 37 °C for 10 min. After half an hour, the first sample was extracted and centrifuged at 13,000 rpm for 30 min at 4 °C. Then, 500 µl of the supernatant was carefully aspirated, and its absorbance was read at 230 nm by UV-Vis spectroscopic analysis (19). The drug release was subsequently measured in the other samples at 2, 4, 6, 16, 24, and 48 hr of incubation.

Cell culture

The cervical cancer cell line HeLa was obtained from the Iranian Genetic Resources Center cell bank. HeLa cells were cultured in Dulbecco's modified Eagle's medium (DMEM) (Gibco - USA) supplemented with 10% (v/v) fetal bovine serum (FBS) (Gibco - USA) and 1% (v/v) penicillin-streptomycin. Cell cultures were maintained in a humidified atmosphere of 5% CO2 at 37 °C (21).

Cytotoxicity assay

Then, the MTT assay was used to evaluate the cytotoxicity of PTX, synthesized AgNPs, and PTX-loaded silver nanoparticles against HeLa cells. Initially, the tumor cells were plated in a 96-well plate with complete medium at a density of 10^4 cells/well and incubated at 37 °C for 24 hr. After incubation, different concentrations (1, 5, 10, 20, 70, 100, 120, 150 µg/mL) of PTX, synthesized AgNPs, and PTX-loaded AgNPs were added to the 96 wells. After 24 hr incubation, 5mg/ml of MTT was added to the tested wells, followed by incubation for 4 hr at 37 °C. After incubation, the treated wells exhibiting formazan crystal formation were diluted with Dimethyl sulfoxide (DMSO). Finally, the color intensity of the wells was read by a spectrophotometer at O.D 570 nm (22).

RNA extraction and real-time PCR

Total RNA was subsequently extracted from the cells 24 hr post-Hela treatment using the RNeasy Mini kit (Qiagen, UK). Subsequently, single-stranded cDNA was synthesized from purified total RNA (Script RT Kit; Qiagen, UK). Real-time PCR reactions were performed on the StepOne device (Applied Biosystems, Foster City, CA, USA). The PCR conditions consisted of 35 cycles at 95 °C for 30s and 65 °C for 60s (23). The primers outlined in Table 1 were employed in this study. The reference gene used was B-actin.

Statistical analysis

Experimental data were reported as mean ± SD using

Table 1. Sequences of forward and reverse primers used for real-time PCR analysis of apoptosis-related genes in treated cancer cells

Gene	Forward	Reverse
β-actin	5'-TCCTCCTGAGCGCAAGTAC-3'	5'-CCTGCTTGCTGATCCACATCT-3'
Bcl-2	5′-ATTGGGAAGTTTCAAATCAGC-3	5′-TCCTCTGTCAAGTTTCCTT-3′
Bax	5'-GAGCTGCAGAGGATGATTGC-3'	5'-AAGTTGCCGTCAGAAAACATG- 3'
Mcl-1	5'-CGCAACCCTCCGGAAGCTG-3'	5'-AAGACCCCGACTCCTTACTG-3'
Caspase-3	5'-GTGCAGACGCGGCTCCTAG-3'	5'-GGTGCAGGGCACACCCAC-3'
Bak	5'-GCGGAGAGCCTGCCCTGCCC-3'	5'-TGGTGCTGCTAGGTTGCAGAG-3'

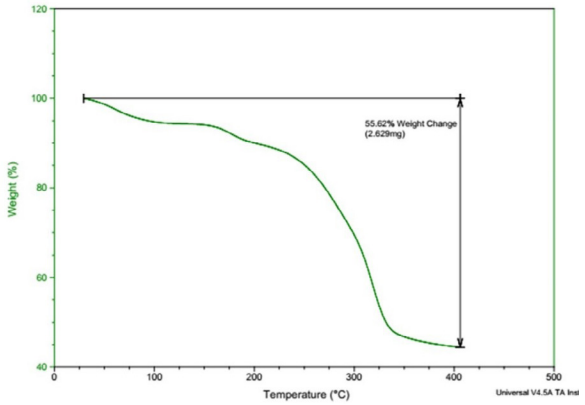

Figure 1. Thermogravimetric analysis (TGA) curve of synthesized silver nanoparticles (AgNPs) showing thermal stability and weight loss profile as a function of temperature

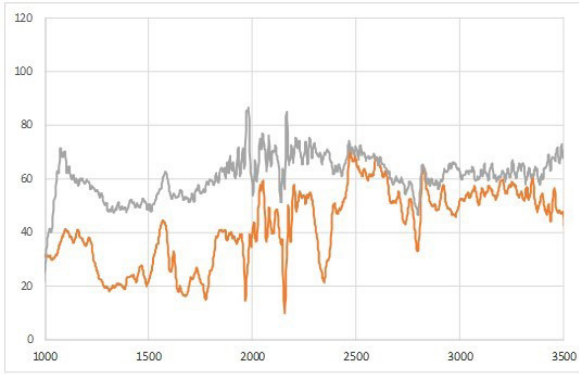

Figure 2. Fourier transform infrared (FTIR) spectra of silver nanoparticles (AgNPs), and paclitaxel-loaded silver nanoparticles (PTX-AgNPs) confirming successful drug loading and interaction between PTX and AgNPs

GraphPad Prism 9. Differences between groups were analyzed by one-way ANOVA followed by Tukey post hoc test. A *P*-value of <0.05 was considered statistically significant. All experiments were performed in triplicate (n=3 independent biological replicates).

Results

Thermogravimetric analysis of AgNPs

A thermogravimetric analysis was done post-synthesis of AgNPs, and the results are presented in Figure 1. There are two distinct stages of weight loss: the first begins at ambient temperature and continues to approximately 150 °C, while the second commences at 150 °C and continues to approximately 400 °C. The first one corresponds to the evaporation of moisture and remaining solvents from nanoparticle synthesis, while the second relates to the destruction of carbon chains, contraction, and upping of chains.

Fourier transform infrared spectroscopy (FTIR)

FTIR is commonly used to study functionalization and to identify bonds. The results for two samples, silver nanoparticle and drug-loaded silver nanoparticle, are shown in Figure 2. In the spectrum of the drug-loaded silver nanoparticle, a peak is observed at 1730 cm^{-1}, indicating the presence of benzamide groups in the sample (gray curve).

Scanning electron microscopy images

SEM imaging shows that the NPs were successfully synthesized in spherical shape. Thus, SEM imaging was used to evaluate NP size. The average size of the synthesized NPs is about 100 nm (Figure 3a). Figures 3b and 3c show the AgNPs and drug-loaded silver nanoparticles.

Study of drug release from paclitaxel-loaded silver nanoparticles

The release of the drug from the loaded NPs was evaluated at 30 min and at 2, 4, 6, 16, 24, and 48 hr after

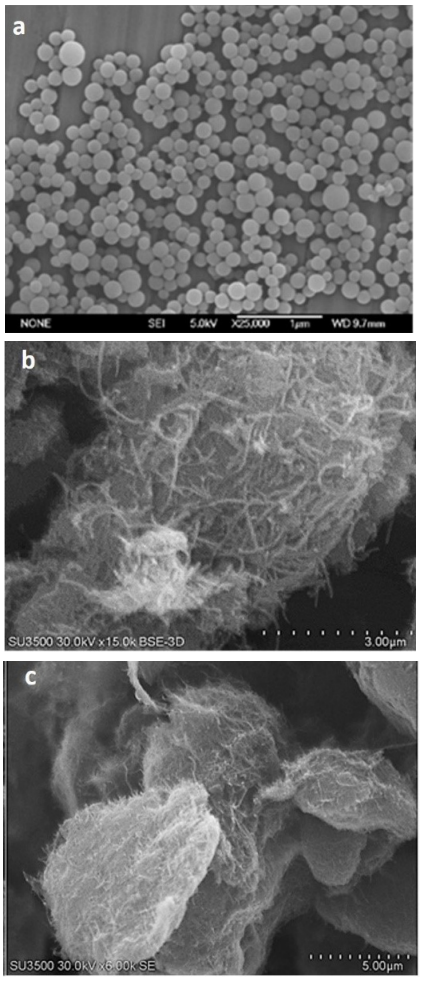

Figure 3. Size of synthesized AgNPs at suitable magnification by SEM (a). Morphological observation of synthesized AgNPs (b) and PTX-loaded AgNPs (c) AgNPs: Silver nanoparticles; PTX: Paclitaxel; SEM: Scanning electron microscope

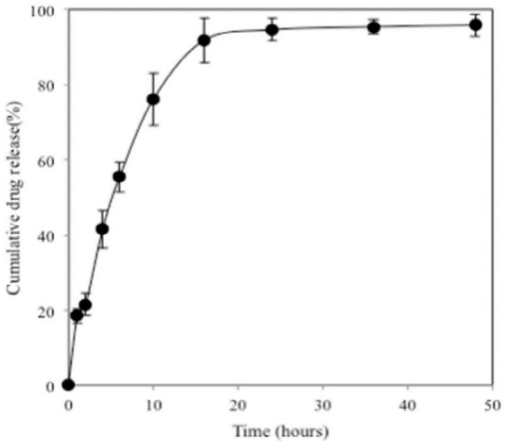

Figure 4. *In vitro* drug release profile of paclitaxel from PTX-AgNPs at 37 °C measured by UV–Vis spectrophotometry at 230 nm, demonstrating a biphasic release pattern with an initial rapid release followed by sustained release up to 48 hr

incubation at 37 °C using a UV–Vis spectrophotometer at 230 nm. The graph below shows the drug release pattern from AgNPs over 48 hr (Figure 4). There are two phases to the release pattern: the first phase is characterized by the rapid release of the drug from NPs, so that 40% of the drug was released from the NPs within 6 hr, while the second phase is characterized by slower release of the remaining drug over 48 hr.

The cytotoxicity pattern of PTX, AgNPs, and PTX-loaded silver nanoparticles in the HeLa cell line.

To evaluate anticancer activity in HeLa cells, cells were treated with varying concentrations of PTX, AgNPs, and PTX-loaded AgNPs for 48 hr. The HeLa cell line showed treatment sensitivity with all factors in a dose-dependent manner. Different doses of PTX, AgNPs, and PTX-loaded AgNPs, including 1, 5, 10, 20, 70, 100, 120, and 150 µg/ml, were further analyzed. Using the MTT assay, the IC_{50} value was calculated at 120 µg/ml for PTX (P=0.0005 vs control, n=3), 100 µg/ml for AgNPs (P=0.0002 vs control, n=3), and 50 µg/ml for PTX-loaded silver nanoparticle (P=0.0001 vs control, F (24,36) =72.88, n=3) in the cell line (Figure 5). As mentioned, PTX-loaded AgNPs significantly induced cell death (IC_{50}) at a lower dose. Doses derived from MTT results were selected (120 µg/ml for PTX, 100 µg/ml for AgNPs, 50 µg/ml for PTX-loaded AgNPs) for molecular studies to reduce the side effects of the anticancer drug.

Gene expression

The Bax/Bcl-2 ratio increased in all the experimental groups after 48 hr treatment compared to the controls; a

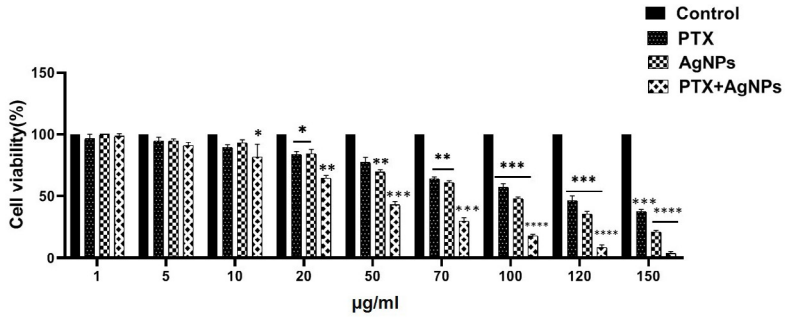

Figure 5. MTT assay of HeLa cells treated with different concentrations of PTX, AgNPs, and PTX-loaded AgNPs (1, 5, 10, 20, 50, 70, 100, 120, and 150 µg/ml) for 48 hr Data shown as mean ± SD (n=3). (*P<0.05, **P<0.01, ***P<0.001, and ****P<0.0001 vs control group). PTX: Paclitaxel; AgNPs: Silver nanoparticles

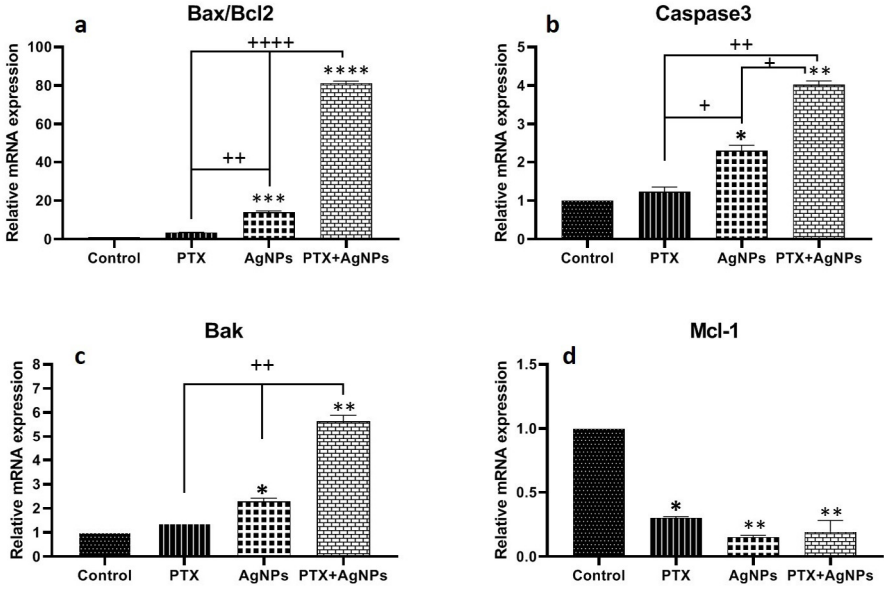

Figure 6. Quantitative real-time PCR analysis of apoptosis-related genes, including Bax/Bcl-2 ratio (a), Caspase-3 (b), Bak (c), and Mcl-1 (d), in HeLa cells after 48 hr treatment, demonstrating significant upregulation of pro-apoptotic markers and downregulation of anti-apoptotic Mcl-1, particularly in the PTX-loaded AgNPs group Data shown as mean ± SD (n=3). *(P<0.05), **(P<0.01), ***P<0.001, and ****P<0.0001 indicate the value significance different from the untreated cells. +(P<0.05), ++(P<0.01), and ++++P<0.0001indicates value significance different from all the other treatments. PTX: Paclitaxel; AgNPs: Silver nanoparticles; Bax: Bcl2 Associated X; Bcl-2: B-cell lymphoma 2

measure for cell death. This was greatest when the PTX-loaded AgNPs were used and resulted in an approximate 81-fold increase in the Bax/Bcl-2 ratio as compared to the control (P<0.0001, vs control, F (3,4) =3689, n=3) (Figure 6a). The most significant expression of Caspase-3, an indicator of apoptosis, was observed in the group given PTX-loaded AgNPs, compared to the control group, about 4 times more than in the control (P=0.0037, vs control, F (3,4) =163.1, n=3) (Figure 6b). Bak (marker of cell death) gene expression has significantly increased in AgNPs about 2-fold (P=0.0273, vs control, n=3) and PTX-loaded AgNPs about 5-fold (P=0.002, vs control, F (3, 4) =129.5, n=3) with respect to the control group. The highest expression rate in HeLa cells was observed in the PTX-loaded AgNPs group (5 times more than the control group) (Figure 6c). Mcl-1 expression level significantly decreased in all treatment groups, comparable between the control group (P=0.0013, vs control, F (3,4) = 80.08, n=3) (Figure 6d). Overall, the results of combination treatment with PTX-loaded AgNPs indicated gene expression favoring apoptosis.

Discussion

Chemoresistance remains a critical challenge in cancer therapy, often rendering chemotherapeutic agents like PTX less effective after prolonged use (24). PTX, a first-line chemotherapeutic agent, promotes tubulin polymerization and inhibits microtubule dynamics, making it a cornerstone in the treatment of cervical cancer (25).

However, the continuous application gives rise to chemoresistance, and drug exposure at high doses causes drug toxicity (26), fostering metastasis instead of inhibiting cell proliferation (27). To address these limitations, combination therapies incorporating NPs, such as silver nanoparticles (AgNPs), have emerged as innovative strategies to enhance anticancer efficacy (28). AgNPs exhibit intrinsic anticancer properties and can serve as carriers for chemotherapeutic agents like PTX (29).

The purpose of this study was to assess the synergistic effects between PTX-loaded AgNPs compared to PTX and AgNPs on HeLa cervical cancer cells regarding cell viability by MTT assay and apoptosis through Real-time PCR analysis of Bax, Bak, Bcl-2, Mcl-1, and caspase-3 gene expression. AgNPs have been synthesized as per the Materials and Methods section. The SEM analysis confirmed their round shape with a size of 100 nm. The dimensions and shapes of AgNPs are crucial determinants of their physical, chemical, and biological properties (30). They influence the surface-to-volume ratio, conductivity, and optical properties (31), with small particles enhancing molecular interactions and penetration into biological systems (32). The 100 nm spherical AgNPs in our study likely contribute to their high penetration and toxicity, as spherical NPs release silver ions more efficiently in terms of their high surface-to-volume ratio, enhancing apoptotic activity by interfering with cellular processes (33). This makes them particularly suitable for biomedical applications due to their facile synthesis and uniformity (34).

We treated HeLa cells with varying doses of AgNPs-PTX (1, 5, 10, 20, 70, 100, 120, and 150 µg/ml) for 48 h and assessed cell cytotoxicity. Our results showed that the combination of PTX and AgNPs synergistically reduced HeLa cell viability and induced apoptosis. IC_{50} values were 120 µg/ml for PTX, 100 µg/ml for AgNPs, and 50 µg/ml for PTX-AgNPs (Figure 5, P<0.001, one-way ANOVA). Real-time PCR data revealed 81-fold upregulation of pro-apoptotic genes Bax/Bcl-2, 4-fold for Caspase-3, and 5-fold for Bak, and 5-fold down-regulation of anti-apoptotic Mcl-1 in PTX-AgNPs-treated cells (Figure 6, P<0.0001), strongly suggesting activation of the intrinsic apoptosis pathway.

Apoptosis, an important mechanism for eliminating tumor cells, is controlled by the Bcl-2 family of proteins, which includes pro-apoptotic Bax and Bak that lower mitochondrial membrane permeability and activate caspases, and anti-apoptotic Bcl-2 and Mcl-1 that inhibit these processes (35-37). PTX, a microtubule-stabilizing drug, induces mitochondrial apoptosis, cell cycle arrest, and cancer cell death (38, 39). Our IC_{50} for PTX (120 µg/ml) is higher than typical values in HeLa cells (42.7 µg/ml in HeLa cells (40)), but aligns with reports using non-DMSO formulations, such as 112.53 µg/ml in HeLa cells (41) and 50µg/ml in MCF-7 cells (19). This high IC_{50} is likely attributable to our water-based PTX formulation (6 mg/ml stock diluted in 2 ml sterile water), which reduces solubility and bioavailability compared to DMSO-based systems.

AgNPs exhibit potent anticancer properties, inducing DNA damage, oxidative stress (42), mitochondrial dysfunction (43), and apoptosis (44) in cancer cells. AgNPs promote apoptosis by increasing cytochrome c release, Bax, caspase-3, and caspase-9 expression, while decreasing anti-apoptotic Bcl-2 levels (45). For instance, AgNPs markedly increased caspase-3 and -7 activity in the bladder cancer cell line (6) and caspase-3 and -9 activity in MCF-7 breast cancer cells (46). An important mechanism of AgNPs is the generation of excessive ROS, a hallmark of cancer cell propagation, which leads to membrane destruction, mitochondrial dysfunction, DNA damage, and oxidative stress-mediated apoptosis (47, 48).

In the present study, IC_{50} for AgNPs (100 µg/ml) is consistent with reports of higher values, such as 200 µg/ml in HeLa cells (49) and 99–165 µg/ml in MDA-MB-231 cells (50), attributed to larger nanoparticle sizes (100 nm in our study, confirmed by SEM) or biosynthetic coatings. In contrast, studies using smaller AgNPs (10–20 nm) report lower IC_{50} (20–50 µg/ml in HeLa cells) (51), highlighting the influence of nanoparticle size and formulation on cytotoxicity.

The alliance of PTX with AgNPs (that is, PTX-AgNPs combination) intensified anticancer potency by damaging the cell nucleus, lysing the cell membrane, producing excessive ROS, damaging mitochondria, and breaking DNA, to be initiated and mediated by caspase-3 activation and a high Bax/Bcl-2 ratio (52). These findings suggested that PTX-AgNPs induce apoptosis via the intrinsic mitochondrial pathway, consistent with the mechanisms of PTX and AgNPs (29, 53).

The synergistic effect of PTX-AgNPs, reducing the IC_{50} to 50 µg/ml, was consistent with the findings of Tutku Tunç *et al.*, who showed AgNPs-PTX increased apoptotic cells by inducing DNA fragmentation and cytotoxic activity in the A549 cell line (16), and Muhammad *et al.* (2021), who observed reduced IC_{50} with PTX-AgNPs in terms of increased reactive oxygen species (ROS) and mitochondrial disruption (52). Our IC_{50} for PTX-AgNPs (50 µg/ml) is lower than that reported by Aygün *et al.* in their 2020 study, which determined an IC_{50} of 165.6 µg/ml for this combination in breast cancer cells (50).

Other PTX-nanoparticle studies, such as Li *et al.* (2016) (54), reported that PTX induces apoptosis of HepG2 cells

through a decrease in mitochondrial membrane potential, DNA fragmentation, and caspase-3 activation, while Rudrappa *et al.* (2020) (55) demonstrated antiproliferative effects of PTX-AgNPs from Plumeria alba in U118 glioblastoma cells. On the other hand, one study using PTX-loaded colorectal NPs in colon cancer cells showed increased expression of Bax and BAD while Bcl-2 was decreased, signaling a pro-apoptotic effect (56); however, this could have been due to their smaller sizes or the DMSO carrier used for PTX. Our observed increases in Bax, Bak, and caspase-3 expression, alongside decreases in Bcl-2 and Mcl-1, align with Muhammad *et al.* (2021), who reported similar gene-expression changes in HeLa cells treated with PTX-AgNPs (52). Similarly, Aborehab *et al.* (2020) (57) and Subramaniam *et al.* (2019) (58) indicated PTX-induced apoptosis in MCF-7 and HeLa cells via Bax and caspase-3 upregulation and Bcl-2 down-regulation. Though other research studies typically will employ direct caspase assays or flow cytometry for Annexin, our study adopted a method relying solely on the MTT assay and Real-time PCR to determine apoptosis following the methodology of Al-Khedhairy *et al.* (2022) (59), Sangour *et al.* (2021) (60), and Aygün *et al.* (2020) (50), who have used similar techniques to demonstrate AgNPs-induced apoptosis in MCF-7 cells and basically any type of breast cancer cell. In summary, our findings showed that PTX-AgNPs enhance apoptosis-induced cell death in HeLa cells, providing a promising strategy to overcome chemoresistance in cervical cancer.

Conclusion

It is possible to enhance the chemosensitivity of HeLa cells using AgNPs and PTX by inducing apoptosis, inhibiting proliferation, and reducing cell survival. Thus, further studies in this direction must focus on *in vivo* models for reaching outcomes that could be termed the final result. In general, these results indicate that AgNPs could be a promising candidate sensitizer for various cancer types, after *in vivo* testing and subsequent validation in clinical trials. Such therapies, especially with PTX, would otherwise be very handy for having an effective combination therapy against cervical cancer.

Acknowledgment

The authors wish to appreciate the financial support of Alborz University of Medical Sciences, Karaj, Iran.

Ethics Approval and Consent to Participate

All experiments were performed in accordance with protocols approved by the Ethics Committee of Alborz University of Medical Sciences.

Availability of Data and Materials

The datasets are available from the corresponding author upon reasonable request.

Funding

The authors declare that no funds, grants, or other support were received during the preparation of this manuscript.

Authors' Contributions

All authors made substantial contributions to the conception and design, acquisition of data, or analysis and interpretation of data. A S designed the study, provided the grant, supervised the study, and prepared the manuscript. M.S helped in statistics and manuscript preparation. M A performed the experiments, gave some interpretations on the results, and manuscript preparation.

Conflicts of Interest

The authors declare no conflicts of interest, financial or otherwise.

Declaration

We have not used any AI tools or technologies to prepare this manuscript.

References

1. Kweik OMA, Hamid MAA, Sheqlieh SO, Abu-Nasser BS, Abu-Naser SS. Artificial neural network for lung cancer detection. Int J Acad Eng Res 2020;4:1-7.
2. Aredo MA, Sendo EG, Deressa JT. Knowledge of cervical cancer screening and associated factors among women attending maternal health services at Aira Hospital, West Wollega, Ethiopia. SAGE Open Med 2021;9:20503121211047063.
3. Walter FM, Mwaka AD, Neal RD. Achieving earlier diagnosis of symptomatic cervical cancer. Br J Gen Pract 2014;64:495–496.
4. Hakim RU, Amin T, Ul Islam SB. Advances and challenges in cervical cancer: From molecular mechanisms and global epidemiology to innovative therapies and prevention strategies. Cancer Control 2025;32:10732748251336415.
5. Alrushaid N, Khan FA, Al-Suhaimi EA, Elaissari A. Nanotechnology in cancer diagnosis and treatment. Pharmaceutics 2023;15:1025.
6. Daei S, Ziamajidi N, Abbasalipourkabir R, Aminzadeh Z, Vahabirad M. Silver nanoparticles exert apoptotic activity in bladder cancer 5637 cells through alteration of Bax/Bcl-2 genes expression. Chonnam Med J 2022;58:102–109.
7. Xiaoxia X, Jing S, Dongbin X, Yonggang T, Jingke Z, Hulai W. Realgar nanoparticles inhibit migration, invasion and metastasis in a mouse model of breast cancer by suppressing matrix metalloproteinases and angiogenesis. Curr Drug Deliv 2020;17:148–158.
8. Wang X, Wang L, Zong S, Qiu R, Liu S. Use of multifunctional composite nanofibers for photothermal chemotherapy to treat cervical cancer in mice. Biomater Sci. 2019;7:3846–3854.
9. Kelly KL, Coronado E, Zhao LL, Schatz GC. The optical properties of metal nanoparticles: the influence of size, shape, and dielectric environment. J Phys Chem B 2003;107:668–677.
10. Ansari MA, Asiri SMM, Alzohairy MA, Alomary MN, Almatroudi A, Khan FA. Biofabricated fatty acids-capped silver nanoparticles as potential antibacterial, antifungal, antibiofilm and anticancer agents. Pharmaceuticals 2021;14:139.
11. Baharara J, Ramezani T, Hosseini N, Mousavi M. Silver nanoparticles synthesized coating with Zataria multiflora leaves extract induced apoptosis in HeLa cells through p53 activation. Iran J Pharm Res 2018;17:627–639.
12. Zenjanab MK, Alimohammadvand S, Doustmihan A, Kianian S, Oskouei BS, Mazloomi M, *et al.* Paclitaxel for breast cancer therapy: A review on effective drug combination modalities and nano drug delivery platforms. J Drug Deliv Sci Technol 2024;95:105567.
13. Alalawy AI. Key genes and molecular mechanisms related to paclitaxel resistance. Cancer Cell Int 2024;24:244.
14. Gasca J, Flores ML, Giráldez S, Ruiz-Borrego M, Tortolero M, Romero F, *et al.* Loss of FBXW7 and accumulation of MCL1 and PLK1 promote paclitaxel resistance in breast cancer. Oncotarget 2016;7:52751–52765.
15. Castilla C, Flores ML, Medina R, Pérez-Valderrama B, Romero F, Tortolero M, *et al.* Prostate cancer cell response to paclitaxel is affected by abnormally expressed securin PTTG1. Mol Cancer Ther 2014;13:2372–2383.
16. Tunç T, Hepokur C, Kariper A. Synthesis and characterization of paclitaxel-loaded silver nanoparticles: Evaluation of cytotoxic

effects and antimicrobial activity. Bioinorg Chem Appl 2024;2024:9916187.
17. Aboul-Nasr MB, Yasien AA, Mohamed SS, Aboul-Nasr YB, Obiedallah M. Exploring the anticancer potential of green silver nanoparticles–paclitaxel nanocarrier on MCF-7 breast cancer cells. Sci Rep 2025;15:20198.
18. Ankireddy K, Iskander M, Vunnam S, Anagnostou DE, Kellar J, Cross W. Thermal analysis of silver nanoparticles for flexible printed antenna fabrication. J Appl Phys 2013;114:124303.
19. Danışman-Kalındemirtaş F, Kariper İA, Hepokur C, Erdem-Kuruca S. Selective cytotoxicity of paclitaxel bonded silver nanoparticle on different cancer cells. J Drug Deliv Sci Technol 2021;61:102265.
20. Baladi M, Amiri M, Amirinezhad M, Abdulsahib WK, Pishgouii F, Golshani Z, *et al*. Green synthesis and characterization of terbium orthoferrite nanoparticles decorated with g-C3N4 for antiproliferative activity. Arab J Chem 2023;16:104841.
21. Amiri M, Basiri M, Eskandary H, Akbarnejad Z, Esmaeeli M, Masoumi-Ardakani Y, *et al*. Cytotoxicity of carboplatin on human glioblastoma cells is reduced by electromagnetic field. Electromagn Biol Med 2018;37:138–145.
22. Yahyapour R, Khoei S, Kordestani Z, Larizadeh MH, Jomehzadeh A, Amirinejad M, *et al*. Comparative study of electromagnetic field and temozolomide administration. Curr Radiopharm 2023;16:123–132.
23. Amirinejad M, Eftekhar-Vaghefi SH, Nematollahi Mahani SN, Salari M, Yahyapour R, Ahmadi-Zeidabadi M. Exposure to low-frequency radiation changes apoptosis markers. Curr Radiopharm 2024;17:55–67.
24. He H, Ni J, Huang J. Molecular mechanisms of chemoresistance in osteosarcoma. Oncol Lett 2014;7:1352–1362.
25. Weaver BA. How Taxol/paclitaxel kills cancer cells. Mol Biol Cell 2014;25:2677–2681.
26. Mokhtari RB, Homayouni TS, Baluch N, Morgatskaya E, Kumar S, Das B, *et al*. Combination therapy in combating cancer. Oncotarget 2017;8:38022–38043.
27. Smith HA, Kang Y. The metastasis-promoting roles of tumor-associated immune cells. J Mol Med 2013;91:411–429.
28. Choudhari AS, Mandave PC, Deshpande M, Ranjekar P, Prakash O. Phytochemicals in cancer treatment. Front Pharmacol 2020;10:1614.
29. Li J, Zhang S, Paik KW, Wong YH, He P, Zhang S. Present status and prospects of nano-silver particles. J Adhes Sci Technol 2025;39:281–318.
30. Kanwar R, Fatima R, Kanwar R, Javid M, Muhammad U, Ashraf Z, *et al*. Biological, physical and chemical synthesis of silver nanoparticles. Pure Appl Biol 2022; 11:418-435
31. Dhaka A, Mali SC, Sharma S, Trivedi R. A review on biological synthesis of silver nanoparticles and their potential applications. Results Chem 2023;6:101108.
32. Kim TH, Kim M, Park HS, Shin US, Gong MS, Kim HW. Size-dependent cellular toxicity of silver nanoparticles. J Biomed Mater Res A 2012;100:1033–1043.
33. Cheon JY, Kim SJ, Rhee YH, Kwon OH, Park WH. Shape-dependent antimicrobial activities of silver nanoparticles. Int J Nanomedicine 2019;14:2773–2780.
34. Raza MA, Kanwal Z, Rauf A, Sabri A, Riaz S, Naseem S. Size- and shape-dependent antibacterial studies of silver nanoparticles synthesized by wet chemical routes. Nanomaterials (Basel) 2016;6:74.
35. Cheng EHY, Kirsch DG, Clem RJ, Ravi R, Kastan MB, Bedi A, *et al*. Conversion of Bcl-2 to a Bax-like death effector by caspases. Science 1997;278:1966–1968.
36. Kang MH, Reynolds CP. Bcl-2 inhibitors: Targeting mitochondrial apoptotic pathways in cancer therapy. Clin Cancer Res 2009;15:1126–1132.
37. Chipuk JE, Green DR. How do BCL-2 proteins induce mitochondrial outer membrane permeabilization? Trends Cell Biol 2008;18:157–164.
38. Alqahtani FY, Aleanizy FS, El Tahir E, Alkahtani HM, AlQuadeib BT. Paclitaxel. Profiles Drug Subst Excip Relat Methodol 2019;44:205–238.
39. Pal MK, Jaiswar SP, Dwivedi A, Goyal S, Dwivedi VN, Pathak AK, *et al*. Synergistic effect of graphene oxide coated nanotised apigenin with paclitaxel. Anticancer Agents Med Chem 2017;17:1721–1732.
40. Kim KS, Cho CH, Park EK, Jung MH, Yoon KS, Park HK. AFM-detected apoptotic changes caused by paclitaxel in HeLa cells. PLoS One 2012;7:e30066.
41. Aborehab NM, Osama N. Effect of gallic acid in potentiating chemotherapeutic effect of paclitaxel in HeLa cervical cancer cells. Cancer Cell Int 2019;19:154.
42. Xin L, Wang J, Fan G, Che B, Wu Y, Guo S, *et al*. Oxidative stress and mitochondrial injury-mediated cytotoxicity induced by silver nanoparticles. Environ Toxicol 2016;31:1691–1699.
43. Holmila RJ, Vance SA, King SB, Tsang AW, Singh R, Furdui CM. Silver nanoparticles induce mitochondrial protein oxidation in lung cells. Antioxidants (Basel) 2019;8:552.
44. Ma J, Di Z, Lu H, Huang W, Yu D. ASK1 activation involved in silver nanoparticle-induced apoptosis of lung cancer cells. J Biomed Nanotechnol 2017;13:349–354.
45. Li J, Chang X, Shang M, Niu S, Zhang W, Zhang B, *et al*. Mitophagy–lysosomal pathway involved in silver nanoparticle-induced apoptosis. Ecotoxicol Environ Saf 2021;208:111463.
46. Ullah I, Khalil AT, Ali M, Iqbal J, Ali W, Alarifi S, *et al*. Green-synthesized silver nanoparticles induce apoptotic cell death in breast cancer cells. Oxid Med Cell Longev 2020;2020:1215395.
47. Chairuangkitti P, Lawanprasert S, Roytrakul S, Aueviriyavit S, Phummiratch D, Kulthong K, *et al*. Silver nanoparticles induce toxicity via ROS-dependent pathways. Toxicol In Vitro 2013;27:330–338.
48. Foldbjerg R, Dang DA, Autrup H. Cytotoxicity and genotoxicity of silver nanoparticles in lung cancer cells. Arch Toxicol 2011;85:743–750.
49. Manivasagan P, Venkatesan J, Senthilkumar K, Sivakumar K, Kim SK. Biosynthesis and cytotoxic effect of silver nanoparticles. Biomed Res Int 2013;2013:287638.
50. Aygün A, Gülbağça F, Nas MS, Alma MH, Çalımlı MH, Ustaoglu B, *et al*. Biological synthesis of silver nanoparticles and anticancer potential. J Pharm Biomed Anal 2020;179:113012.
51. Yuan YG, Zhang S, Hwang JY, Kong IK. Silver nanoparticles potentiate cytotoxicity in cervical cancer cells. Oxid Med Cell Longev 2018;2018:6121328.
52. Muhammad N, Zhao H, Song W, Gu M, Li Q, Liu Y, *et al*. Silver nanoparticles functionalized paclitaxel nanocrystals enhance anticancer effect. Nanotechnology. 2021;32:085105.
53. Rose PG, Blessing JA, Gershenson DM, McGehee R. Paclitaxel and cisplatin as first-line therapy in cervical cancer. J Clin Oncol. 1999;17:2676–2680.
54. Li Y, Guo M, Lin Z, Zhao M, Xiao M, Wang C, *et al*. Silver nanoparticle-based co-delivery of paclitaxel induces apoptosis. Int J Nanomedicine. 2016;11:6693–6702.
55. Rudrappa M, Rudayni HA, Assiri RA, Bepari A, Basavarajappa DS, Nagaraja SK, *et al*. Green synthesis of silver nanoparticles exhibits anticancer activity. Nanomaterials (Basel). 2022;12:493.
56. Alsadooni JFK, Haghi M, Barzegar A, Feizi MAH. Chitosan hydrogel containing nanoparticle complex with paclitaxel on cancer cells. Int J Biol Macromol. 2023;247:125612.
57. Aborehab NM, Elnagar MR, Waly NE. Gallic acid potentiates apoptotic effect of paclitaxel via Bax overexpression. J Biochem Mol Toxicol. 2021;35:e22638.
58. Subramaniam Y, Subban K, Chelliah J. Synergistic anticancer effect of fungal compound and paclitaxel in cervical cancer. Toxicol In Vitro 2021;72:105079.
59. Al-Khedhairy AA, Wahab R. Silver nanoparticles anticancer activity against liver and breast cancer cells. Metals (Basel) 2022;12:148.
60. Sangour MH, Ali IM, Atwan ZW, Al Ali AAALA. Effect of Ag nanoparticles on viability of MCF-7 and Vero cell lines and gene expression of apoptotic genes. Egypt J Med Hum Genet 2021;22:9.